

# GMTR: GRAPH MATCHING TRANSFORMERS

Jinpei Guo, Shaofeng Zhang, Runzhong Wang, Chang Liu, Junchi Yan\*

MOE Key Lab of Artificial Intelligence, Shanghai Jiao Tong University, Shanghai, China

## ABSTRACT

Vision transformers (ViTs) have recently been used for visual matching. The original grid dividing strategy of ViTs neglects the spatial information of the keypoints, limiting the sensitivity to local information. We propose **QueryTrans** (Query Transformer), which adopts a cross-attention module and keypoints-based center crop strategy for better spatial information extraction. We further integrate the graph attention module and devise a transformer-based graph matching approach **GMTR** (Graph Matching TRANSformers) whereby the combinatorial nature of GM is addressed by a graph transformer GM solver. On standard GM benchmarks, GMTR shows competitive performance against the SOTA frameworks. Specifically, on Pascal VOC, GMTR achieves **83.6%** accuracy, **0.9%** higher than the SOTA. On SPair-71k, GMTR shows great potential and outperforms most of the previous works. Meanwhile, on Pascal VOC, QueryTrans improves the accuracy of NGMv2 from 80.1% to **83.3%**, and BBGM from 79.0% to **84.5%**. On SPair-71k, it improves NGMv2 from 80.6% to **82.5%**, and BBGM from 82.1% to **83.9%**. Code is available at: <https://github.com/jp-guo/gm-transformer>.

**Index Terms**— graph matching, vision transformers

## 1. INTRODUCTION AND RELATED WORK

Since the debut of Vision Transformer (ViT) [1], variant transformers [2, 3] have been devised to handle different vision tasks (e.g., DETR [4] on detection and SETR [3] on segmentation) and outperform ConvNets. However, when applying transformers to visual graph matching, a standard spatial-sensitive task involving keypoints matching, the grid dividing design in ViTs omits the keypoints spatial information and therefore poses a significant limitation to the performance of transformers. Hence, exploring the potential of transformers in visual graph matching remains open.

Visual GM extracts keypoint features and model their relation from images, and aims to find the correspondence between two or multiple images, which is essentially NP-hard with wide applications in vision. Most existing visual GM methods [5, 6, 7, 8] adopt the ConvNets (e.g., VGGs and ResNets) to extract keypoint information, where CNNs are shown to be less competitive to **relational modeling** [9] (e.g. convolution

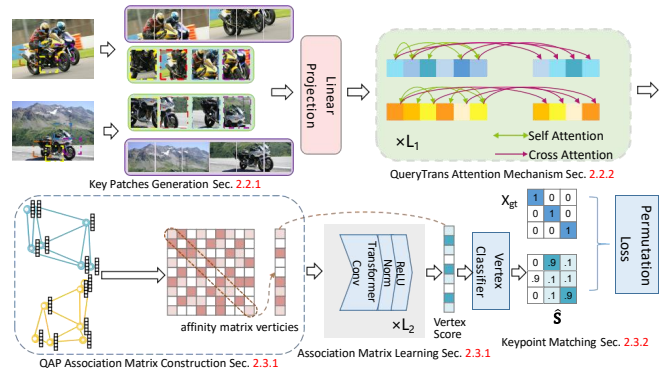


**Fig. 1.** Overview of GMTR. The frontend QueryTrans extracts image features via generated raw patches and key patches (region crops around keypoints), followed with self-attention and cross-attention layers. The affinity matrix as input instance, is then tackled by the backend transformer. All modules are end-to-end trained with the permutation loss [6].

for sequential data). To solve the two bottlenecks (less spatial sensitiveness and relational modeling), we propose QueryTrans (Query Transformer), integrating transformers in visual GM and solving the spatial-insensitive problem for ViTs. We split the image into patches (raw patches). For each keypoint, we crop a region around the keypoint (key patches) with the same size of raw patches followed by the vision transformer.

Previous works have applied the transformers to image matching and show promising potential. While graph matching refers to keypoint to keypoint matching of graph structure, [10, 11] focus on dense pixel to pixel matching of images, which show few strengths on graph structure. Instead of straightforwardly borrowing transformers in our approach, we exploit the graph structure and design a cross attention mechanism between raw patches and key patches to decrease the bias for better localized keypoints information. Following [7] that treats the NP-hard quadratic assignment problem (QAP) solving as a vertex classification task, we naturally replace GNNs with transformers to exploit the mutual information in the graph structure and explore their potential in solving combinatorial optimization problems. By introducing the key patches, cross attention mechanism, and the transformer GM solver, GMTR achieves new SOTA results on standard visual graph matching datasets Pascal VOC (with Berkeley annotations [12]) and exhibits great potential on SPair-71k [13].

**The contributions are summarized as follows:** 1) We

\*Corresponding author. Work was supported by National Key Research and Development Project (2020AAA0107600) and NSFC (6222607).

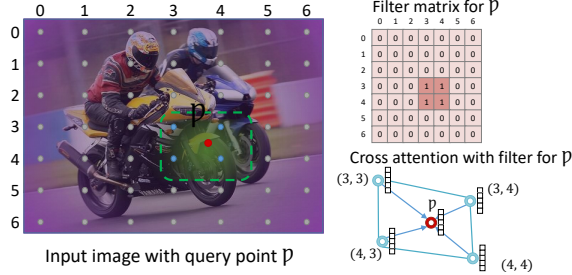


**Fig. 2.** Illustration of filter matrix  $\mathbf{D}$  used in our devised QueryTrans for the query point  $\mathcal{P}$  for keypoint feature learning, which conducts message passing with neighboring 4 patches. Each grey point the center of raw patches, red point denotes the center of query patches, blue points the center of neighboring raw patches for query patches. See details in Sec. 2.2.2.

propose a transformer-based method namely Graph Matching Transformers (GMTR) to improve the relational modeling and further exploit the property of graph structure. 2) We devise techniques including raw/key patch cross attention and center region crop for better keypoint feature extraction, improving the sensitivity over original ViTs. 3) We conduct comprehensive experiments on popular GM benchmarks which prove the strengths of our proposed methods on all the datasets.

## 2. THE PROPOSED METHOD

### 2.1. Preliminaries: Vision Transformers

For image  $\mathbf{x} \in \mathbb{R}^{C \times H \times W}$ , where  $H \times W$  is the resolution of the image and  $C$  is the number of channels, ViT [1] treats the image  $\mathbf{x}$  as a sequence composed of non-overlapping patches  $\{\mathbf{x}^{(i)} \in \mathbb{R}^{C \times P^2}\}_{i=1}^N$ , where each patch has a fixed  $P \times P$  resolution. Then, the patches are linearly transformed to  $D$ -dimensional patch embeddings  $\mathbf{z}^{(i)} = \mathbf{E}\mathbf{x}^{(i)} + \mathbf{W}_{pos}^i \in \mathbb{R}^D$ , where  $\mathbf{E} \in \mathbb{R}^{D \times C \times P^2}$  is the linear projection and  $\mathbf{W}_{pos} \in \mathbb{R}^D$  is the positional embedding for the  $i$ -th patch. A  $[CLS]$  token  $\mathbf{z}^{[CLS]} \in \mathbb{R}^D$  is subsequently prepended to the patch sequence to extract global information, so the resulting input sequence is represented as  $\mathbf{z} = [\mathbf{z}^{[CLS]}, \mathbf{z}^{(1)}, \mathbf{z}^{(2)}, \dots, \mathbf{z}^{(N)}]$ . Then, ViT uses a transformer encoder to generate both image-level ( $[CLS]$  token) and patch-level (other tokens). In line with [1], we use  $f_\theta$  to denote the process of a ViT parameterized by  $\theta$ :

$$\begin{aligned} f_\theta(\mathbf{x}) &= f_\theta \left( [\mathbf{z}^{[CLS]}, \mathbf{z}^{(1)}, \mathbf{z}^{(2)}, \dots, \mathbf{z}^{(N)}] \right) \\ &= [f_\theta^{[CLS]}(\mathbf{x}), f_\theta^{(1)}(\mathbf{x}), f_\theta^{(2)}(\mathbf{x}), \dots, f_\theta^{(N)}(\mathbf{x})], \end{aligned} \quad (1)$$

where  $f_\theta^{[CLS]}(\mathbf{x})$  and  $f_\theta^{(i)}(\mathbf{x})$  are the representations of the whole image and the  $i$ -th patch, respectively.

### 2.2. Frontend: Query Transformer

#### 2.2.1. Key patches generation

ViT's spatial insensitivity can limit its ability to extract keypoint information, which may negatively impact its performance in GM tasks. As a remedy, we propose creating patches

around keypoints to improve expressiveness. Specifically, as shown in top left of Fig. 1, for each keypoint, we crop a region with the same size of raw patches (e.g.,  $8 \times 8$ ,  $16 \times 16$ ) followed by the patch embedding layer, as formulated by:

$$\mathbf{p}^{[(N+1), \dots, (N+K)]} = \text{PatchEmbed} \left( \mathbf{x}^{[(N+1), \dots, (N+K)]} \right) \quad (2)$$

where  $\mathbf{p}^{[(N+1), \dots, (N+K)]}$  means a sequence composed of the key patches embeddings. For distinguish, we call the patches generated by original ViT as **raw** patches and those patches generated by region crop around keypoints as **key** patches. Then, the input embeddings can be formulated as:

$$\mathbf{z} = \left[ \mathbf{z}^{[CLS]}, \underbrace{\mathbf{z}^{(1)}, \mathbf{z}^{(2)}, \dots, \mathbf{z}^{(N)}}_{\text{raw patches}}, \underbrace{\mathbf{z}^{(q_1)}, \mathbf{z}^{(q_2)}, \dots, \mathbf{z}^{(q_Q)}}_{\text{key patches}} \right]. \quad (3)$$

Note that  $\mathbf{z}^{[CLS]}$  and raw patches  $[\mathbf{z}^{(1)}, \mathbf{z}^{(2)}, \dots, \mathbf{z}^{(N)}]$  will be equipped with positional embeddings.

#### 2.2.2. Cross attention mechanism with filter module

Instead of directly feeding the whole sequence (namely  $[CLS]$  token, raw patches, query patches) to the transformer encoder, which may hurt the performance of the finetuning on GM task (as only  $[CLS]$  token and raw patches are fed to the transformer for pretraining), we modify the attention mechanism as follows. Specifically, given one  $\mathbf{z}^{[CLS]}$  token, raw patches sequence  $[\mathbf{z}^{(1)}, \mathbf{z}^{(2)}, \dots, \mathbf{z}^{(N)}]$  and query patches sequence  $[\mathbf{z}^{(q_1)}, \mathbf{z}^{(q_2)}, \dots, \mathbf{z}^{(q_Q)}]$ . Let  $\mathbf{z}' = [\mathbf{z}^{[CLS]}, \mathbf{z}^{(1)}, \mathbf{z}^{(2)}, \dots, \mathbf{z}^{(N)}]$  and  $\mathbf{z}^q = [\mathbf{z}^{(q_1)}, \mathbf{z}^{(q_2)}, \dots, \mathbf{z}^{(q_Q)}]$ . For  $\mathbf{z}^{[CLS]}$  and raw patches, the propagation rule in the attention block is in line with vision transformer, i.e.,

$$\text{Attn}(\mathbf{Q}_{\mathbf{z}'}, \mathbf{K}_{\mathbf{z}'}, \mathbf{V}_{\mathbf{z}'}) = \text{Softmax} \left( \frac{\mathbf{Q}_{\mathbf{z}'} \mathbf{K}_{\mathbf{z}'}^\top}{\sqrt{d_k}} \right) \mathbf{V}_{\mathbf{z}'}, \quad (4)$$

where  $\mathbf{Q}_{\mathbf{z}'} = \mathbf{z}' \mathbf{W}_Q$ ,  $\mathbf{K} = \mathbf{z}' \mathbf{W}_K$ ,  $\mathbf{V} = \mathbf{z}' \mathbf{W}_V$ , with learnable weights  $\mathbf{W}_Q$ ,  $\mathbf{W}_K$ ,  $\mathbf{W}_V$ . For query patches  $\mathbf{z}^{(q_i)}$ , the attention propagation rule is similar to  $[CLS]$  token, i.e.,

$$\text{Attn}(\mathbf{Q}_{\mathbf{z}^{(q_i)}}, \mathbf{K}_{\mathbf{z}'}, \mathbf{V}_{\mathbf{z}'}) = \text{Softmax} \left( \frac{\mathbf{Q}_{\mathbf{z}^{(q_i)}} \mathbf{D} \mathbf{K}_{\mathbf{z}'}^\top}{\sqrt{d_k}} \right) \mathbf{V}_{\mathbf{z}'}, \quad (5)$$

where  $\mathbf{Q}_{\mathbf{z}^{(q_i)}} = \mathbf{z}^{(q_i)} \mathbf{W}_Q$  and  $\mathbf{D}$  is the filter module as:

$$\mathbf{D}_{ij} = \begin{cases} 1, & |i - j| \leq 1 \\ 0, & |i - j| > 1 \end{cases} \quad (6)$$

For illustration, we visualize the construction of filter matrix  $\mathbf{D}$  for one specific query point  $\mathcal{P}$  in Fig. 2.

By Eq. 4 and Eq. 5, we complete the attention block in the modified transformer. By Eq. 5, we derive the keypoint embeddings  $[\mathbf{Z}^{(q_1)}, \mathbf{Z}^{(q_2)}, \dots, \mathbf{Z}^{(q_Q)}]$ . To fully use the spatial information, we also use bilinear algorithm in the raw patch embeddings  $\mathbf{Z}^b = [\mathbf{Z}^{(b_1)}, \mathbf{Z}^{(b_2)}, \dots, \mathbf{Z}^{(b_Q)}]$  of the final output layer, as also commonly used in previous GM methods [6]. Then, the final keypoint embeddings are:  $\mathbf{Z} = \text{Concat}(\mathbf{Z}^q, \mathbf{Z}^b)$ .

**Table 1.** Average accuracy (%) of each object on Pascal VOC.

model	aero	bike	bird	boat	bottle	bus	car	cat	chair	cow	table	dog	horse	motor	person	plant	sheep	sofa	train	tv	Avg
GMN [5]	31.9	47.2	51.9	40.8	68.7	72.2	53.6	52.8	34.6	48.6	72.3	47.7	54.8	51.0	38.6	75.1	49.5	45.0	83.0	86.3	55.3
PCA [6]	49.8	61.9	65.3	57.2	78.8	75.6	64.7	69.7	41.6	63.4	50.7	67.1	66.7	61.6	44.5	81.2	67.8	59.2	78.5	90.4	64.8
NGM [7]	50.1	63.5	57.9	53.4	79.8	77.1	73.6	68.2	41.1	66.4	40.8	60.3	61.9	63.5	45.6	77.1	69.3	65.5	79.2	88.2	64.1
IPCA [6]	53.8	66.2	67.1	61.2	80.4	75.3	72.6	72.5	44.6	65.2	54.3	67.2	67.9	64.2	47.9	84.4	70.8	64.0	83.8	90.8	67.7
CIE [8]	52.5	68.6	70.2	57.1	82.1	77.0	70.7	73.1	43.8	69.9	62.4	70.2	70.3	66.4	47.6	85.3	71.7	64.0	83.8	91.7	68.9
BBGM [14]	61.9	71.1	79.7	79	87.4	94	89.5	80.2	56.8	79.1	64.6	78.9	76.2	75.1	65.2	98.2	77.3	77	94.9	93.9	79.0
NGMv2 [7]	61.8	71.2	77.6	78.8	87.3	93.6	87.7	79.8	55.4	77.8	89.5	78.8	80.1	79.2	62.6	97.7	77.7	75.7	96.7	93.2	80.1
ASAR [15]	62.9	74.3	79.5	80.1	89.2	94.0	88.9	78.9	58.8	79.8	88.2	78.9	79.5	77.9	64.9	98.2	77.5	77.1	98.6	93.7	81.1
COMMON [16]	65.6	75.2	80.8	79.5	89.3	92.3	90.1	81.8	61.6	80.7	95.0	82.0	81.6	79.5	66.6	98.9	78.9	80.9	99.3	93.8	82.7
GMTR (Ours)	69.0	74.2	84.1	75.9	87.7	94.2	90.9	87.8	62.7	83.5	93.9	84.0	78.7	79.6	69.2	99.3	82.5	83.0	99.1	93.3	<b>83.6</b>

**Table 2.** Average accuracy (%) of each object on SPair-71k.

model	aero	bike	bird	boat	bottle	bus	car	cat	chair	cow	dog	horse	motor	person	plant	sheep	train	tv	Avg
GMN [5]	59.9	51.0	74.3	46.7	63.3	75.5	69.5	64.6	57.5	73.0	58.7	59.1	63.2	51.2	86.9	57.9	70.0	92.4	65.3
PCA [6]	64.7	45.7	78.1	51.3	63.8	72.7	61.2	62.8	62.6	68.2	59.1	61.2	64.9	57.7	87.4	60.4	72.5	92.8	66.0
NGM [7]	66.4	52.6	77.0	49.6	67.7	78.8	67.6	68.3	59.8	73.6	63.9	60.7	70.7	60.9	87.5	63.9	79.8	91.5	68.9
IPCA [6]	69.0	52.9	80.4	54.3	66.5	80.0	68.5	71.4	61.4	74.8	66.3	65.1	69.6	63.9	91.1	65.4	82.9	97.5	71.2
CIE [8]	71.5	57.1	81.7	56.7	67.9	82.5	73.4	74.5	62.6	78.0	68.7	66.3	73.7	66.0	92.5	67.2	82.3	97.5	73.3
BBGM [14]	72.5	64.6	87.8	75.8	69.3	94.0	88.6	79.9	74.6	83.2	78.8	77.1	76.5	76.3	98.2	85.5	96.8	99.3	82.1
NGMv2 [7]	68.8	63.3	86.8	70.1	69.7	94.7	87.4	77.4	72.1	80.7	74.3	72.5	79.5	73.4	98.9	81.2	94.3	98.7	80.2
ASAR [15]	72.4	61.8	91.8	79.1	71.2	97.4	90.4	78.3	74.2	83.1	77.3	77.0	83.1	76.4	99.5	85.2	97.8	99.5	83.1
COMMON [16]	77.3	68.2	92.0	79.5	70.4	97.5	91.6	82.5	72.2	88.0	80.0	74.1	83.4	82.8	99.9	84.4	98.2	99.8	<b>84.5</b>
GMTR (Ours)	75.6	67.2	92.4	76.9	69.4	94.8	89.4	77.5	72.1	86.3	77.5	72.2	86.4	79.5	99.6	84.4	96.6	99.7	83.2

### 2.3. Backend: GM Solver Transformer

#### 2.3.1. Association matrix learning

In QAP, the association matrix contains the first order (node-to-node similarity) and second order (edge-to-edge similarity) information of two graphs. We follow the method of [7] to construct the association matrix with the keypoint features extracted from the frontend module (e.g. QueryTrans). We derive the node embeddings from the association matrix (i.e. association matrix learning) with the backend modules. In contrast with the previous works [6, 7, 14], we apply the graph transformer TransformerConv [17] for association matrix learning, since TransformerConv has shown strengths on both graph-level and node-level prediction tasks over graph convolution networks [18] and other transformer graph networks [19, 20]. Small parameters and simple yet effective pipeline furthermore improve the transferability to combinatorial optimization problem. Specifically, we use  $\mathbf{K}_p \in \mathbb{R}^{n_1 \times n_2 \times d}$  and  $\mathbf{K} \in \mathbb{R}^{n_1 n_2 \times n_1 n_2 \times d}$  to denote the node similarity matrix and the association matrix, respectively. we view  $\text{vec}(\mathbf{K}_p)$  as the node feature, and  $\mathbf{K}$  as the edge attribute in TransformerConv. The attention in each layer is calculated as:

$$\text{attn}_{ij}^l = \text{Softmax}_{j \in \mathcal{N}(i)} \left( \frac{\mathbf{q}_i^l (\mathbf{k}_j^l{}^\top + \mathbf{e}_{ij}^l)}{\sqrt{d}} \right) \quad (7)$$

where  $\mathcal{N}(i)$  denotes the neighbor of node  $i$ , namely  $\mathbf{W}_{ij} > 0$  if  $j \in \mathcal{N}(i)$ .  $\mathbf{q}^l = \mathbf{z}^l \mathbf{W}_Q^l$ ,  $\mathbf{k}^l = \mathbf{z}^l \mathbf{W}_K^l$ ,  $\mathbf{e}^l = \mathbf{K} \mathbf{W}_e^l$ ,  $\mathbf{z}^l$  is the node feature of the  $l$ -th TransformerConv layer.

We make message aggregation for each node as follows:

$$\mathbf{z}_i^{l+1} = \text{ReLU}(\text{LayerNorm}(\text{attn}_{ij}^l \cdot (\mathbf{v}_j^l + \mathbf{e}_{ij}^l))) \quad (8)$$

where,  $\mathbf{v}^l = \mathbf{z}^l \mathbf{W}_V^l$ . Specifically, for the last layer, we adopt multi-head attention mechanism, where the activation function

**Table 3.** Average accuracy (%) with combination of backbones under two baseline frameworks: NGMv2 and BBGM.

Backbone	Pascal VOC		SPair-71k	
	NGMv2	BBGM	NGMv2	BBGM
VGG16 [22]	80.1	79.0	80.6	82.1
ResNet34 [23]	80.2	80.7	80.4	81.5
ViT [1]	82.7	83.6	80.8	83.0
CeIT [24]	82.6	83.1	81.6	81.4
XCIIT [25]	82.7	82.8	81.7	82.3
QueryTrans (Ours)	<b>83.3</b>	<b>84.5</b>	<b>82.5</b>	<b>83.9</b>

and normalization layer are abandoned.

$$\mathbf{z}_i^k = \frac{1}{H} \sum_{i=1}^C \text{attn}_{c,ij}^l (\mathbf{v}_{c,j}^l + \mathbf{e}_{c,ij}^l) \quad (9)$$

#### 2.3.2. Keypoint matching

We obtain the node embedding  $\mathbf{z}^{final} \in \mathbb{R}^{n_1 n_2 \times d}$  by Eq. 9. We project the embedding with an FC layer:  $\mathbf{m} = \mathbf{z}^{final} \times \mathbf{W}_{proj}$ , where  $\mathbf{W}_{proj} \in \mathbb{R}^{d \times 1}$  is a learnable parameter. Inspired by [5, 6], we adopt a Sinkhorn network [21]  $f : \mathbb{R}^{n_1 n_2 \times 1} \rightarrow [0, 1]^{n_1 \times n_2}$  to calculate the matching.

As each entry in matching matrix can be regarded as a binary classification where 1 denotes matched and 0 denotes unmatched, we adopt binary cross-entropy as our loss function. Given matching ground truth  $\mathbf{X}^{gt}$ , the loss is:

$$\mathcal{L} = - \frac{\sum_{i=1}^{n_1} \sum_{j=1}^{n_2} (\mathbf{X}_{ij}^{gt} \log(\mathbf{m}_{ij}) + (1 - \mathbf{X}_{ij}^{gt}) \log(1 - \mathbf{m}_{ij}))}{n_1 n_2}$$

Please note that our backend module can solve the QAP independently without the front-end module since the only input is the QAP affinity matrix, which is, to our best knowledge, the first successful application for transformer in Lawler’s Quadratic Assignment Problem (QAP).

### 3. EXPERIMENTS

#### 3.1. Overall Performance on Pascal VOC

We conduct experiments on Pascal VOC, which consists of 20 instance classes, with each image containing 6 to 23 key points. To compare our model with peer approaches, we follow the same settings as previous works [6, 7, 14], which involve filtering the outlier points to guarantee only the points present in both source image and target image are preserved. Images are then re-scaled according to the frontend. Results are given in Table 1. GMTR achieves the SOTA performance.

#### 3.2. Overall Performance on SPair-71k

SPair-71k is a large dataset consisting of 70,958 image pairs with diverse variations in viewpoint and scale. Compared to Pascal VOC dataset, it is large in number and contains more annotations. We follow the same setting as in the previous section, select intersection points, and each image is cropped to its bounding box and scaled to  $256 \times 256$  or  $224 \times 224$ . Table 2 indicates that GMTR shows strengths on SPair-71k as well, outperforming most of the peer works.

#### 3.3. Ablation Study

##### 3.3.1. Study on Backbones

We test CNN-based and transformer-based backbones under the NGMv2 and BBGM frameworks on Pascal VOC and SPair-71k. For CNN-based, we test VGG16 [22] and ResNet34 [23], which are two classical models. For transformer-based model, we conduct experiments on ViT [1], CeiT [24] and XcIT [25], which show competitive performance on ImageNet1k. Finally, we test our QueryTrans, which adopts both self-attention and cross-attention mechanism to extract information. All other parameters irrelevant to the backbone and image rescale values ( $256 \times 256$  or  $224 \times 224$ ) are kept constant across all models. The results are shown in Table 3.

**Results on Pascal VOC dataset:** For both NGMv2 and BBGM frameworks, we set learning rate  $2 \times 10^{-5}$  for backbone training and  $2 \times 10^{-3}$  for other modules. The backend modules are implemented using a 3-layer GCN [18], whose feature dimension is 16. The results show that our proposed QueryTrans performs the best under both frameworks.

**Results on SPair-71k:** We test QueryTrans and previous mentioned CNN-based and transformer-based backbones with NGMv2 and BBGM on SPair-71k. The learning rate is set as  $1 \times 10^{-5}$  for backbones and  $1 \times 10^{-3}$  for other modules. The results indicate that QueryTrans outperforms all the backbones under both frameworks on SPair-71k dataset.

##### 3.3.2. Study on TransformerConv Modules

We conduct experiments to show the strengths of TransformerConv [17] over GNNs (e.g. GCN [18]). The number of GCN layers is set as 3, with feature dimension of 17 (16 + Sinkhorn [21]). The number of TransformerConv layers is 3, with feature dimension of 16. We adopt multi-head self attention where the number of heads for each layer is 1, 1, and 2 respectively. To verify the necessity of backend module, we

**Table 4.** Ablation study of the variants of backend modules.

Exp.	Setup (on Pascal VOC dataset)	accuracy
A	baseline(QueryTrans + TransformerConv + positional encoding)	83.63
B	A - TransformerConv + GCN	83.28
C	A - TransformerConv	73.09
D	A - positional encoding	76.12
E	B - positional encoding	75.08

**Table 5.** Ablation study of image information extract method based on vision transformer on Pascal VOC dataset.

Method	Accuracy	Relative acc
bilinear (ViT)	82.68	0
cross-attention	77.98	-4.70
cross-attention + filter	81.88	-0.80
bilinear + corss-attention	79.26	-3.42
bilinear + cross-attention + filter	83.63	+0.95

also test the performance without backend module. The node information is directly passed to the final layer.

In Table 4, Exp. A & B show that the attention mechanism combined with the association graph is more effective in updating node features and capturing the relationships between nodes and their neighbors. Exp. C highlights the necessity of the backend module. Exp. D & E show that positional encoding is crucial for both GCN and TransformerConv.

##### 3.3.3. Study on Attention with Filter

One key design of our QueryTrans is the filter, which masks the raw patches that contain no overlapping area with the query patch. We conduct experiments to demonstrate the necessity of the filter. We also explore the performance of different node embedding designs. Specifically, **bilinear** means the model adopts the bilinear algorithm over raw patches from the last two layers of QueryTrans, and concatenates the two vectors as node feature. **Cross-attention** means the model concatenates the query patches from the last two layers of QueryTrans as the output. **cross-attention+bilinear** denotes the model adopts the bilinear algorithm over raw patches from the last layer of QueryTrans, and concatenate them with query patches from the last layer of QueryTrans as the output. The results are given in Table 5, where **cross-attention+bilinear+filter** performs the best, indicating that local query information combined with spatial information provides more accurate features.

## 4. CONCLUSION

We have proposed GMTR, a transformer-based approach for visual graph matching, with two key components, i.e., QueryTrans and a backend transformer, where QueryTrans learns the visual keypoints information from keypoint crops and cross attention mechanism, and the backend transformer further improves the matching accuracy. Moreover, QueryTrans can be integrated into popular GM frameworks (NGMv2, BBGM). Extensive experimental results on popular GM benchmarks show that GMTR achieves competitive performance.

## 5. REFERENCES

- [1] Alexey Dosovitskiy, Lucas Beyer, Alexander Kolesnikov, Dirk Weissenborn, Thomas Unterthiner Xiaohua Zhai, Matthias Minderer Mostafa Dehghani, Sylvain Gelly Georg Heigold, Jakob Uszkoreit, and Neil Houlsby, “An image is worth 16x16 words: Transformers for image recognition at scale,” in *ICLR*, 2021.
- [2] Ze Liu, Yutong Lin, Yue Cao, Han Hu, Yixuan Wei, Zheng Zhang, Stephen Lin, and Baining Guo, “Swin transformer: Hierarchical vision transformer using shifted windows,” in *ICCV*, 2021, pp. 10012–10022.
- [3] Sixiao Zheng, Jiachen Lu, Hengshuang Zhao, Xiatian Zhu, Zekun Luo, Yabiao Wang, Yanwei Fu, Philip H.S. Torr Jianfeng Feng, Tao Xiang, and Li Zhang, “Rethinking semantic segmentation from a sequence-to-sequence perspective with transformers,” in *CVPR*, 2021.
- [4] Nicolas Carion, Francisco Massa, Gabriel Synnaeve, Nicolas Usunier, Alexander Kirillov, and Sergey Zagoruyko, “End-to-end object detection with transformers,” in *ECCV*, 2020.
- [5] Andrei Zanfir and Christian Sminchisescu, “Deep learning of graph matching,” in *CVPR*, 2018, pp. 2684–2693.
- [6] Runzhong Wang, Junchi Yan, and Xiaokang Yang, “Learning combinatorial embedding networks for deep graph matching,” in *ICCV*, 2019, pp. 3056–3065.
- [7] Runzhong Wang, Junchi Yan, and Xiaokang Yang, “Neural graph matching network: Learning lawler’s quadratic assignment problem with extension to hypergraph and multiple-graph matching,” *IEEE TPAMI*, 2022.
- [8] Tianshu Yu, Runzhong Wang, Junchi Yan, and Baoxin Li, “Learning deep graph matching with channel-independent embedding and hungarian attention,” in *ICLR*, 2020.
- [9] Vijay Prakash Dwivedi and Xavier Bresson, “A generalization of transformer networks to graphs,” *arXiv preprint arXiv:2012.09699*, 2020.
- [10] Paul-Edouard Sarlin, Daniel DeTone, Tomasz Malisiewicz, and Andrew Rabinovich, “Superglue: Learning feature matching with graph neural networks,” in *CVPR*, 2020.
- [11] Jiaming Sun, Zehong Shen, Yuang Wang, Hujun Bao, and Xiaowei Zhou, “Loftr: Detector-free local feature matching with transformers,” in *CVPR*, 2021.
- [12] Lubomir Bourdev and Jitendra Malik, “Poselets: Body part detectors trained using 3d human pose annotations,” in *ICCV*, 2009, pp. 1365–1372.
- [13] Juhong Min, Jongmin Lee, Jean Ponce, and Minsu Cho, “Spair-71k: A large-scale benchmark for semantic correspondence,” *arXiv preprint arXiv:1908.10543*, 2019.
- [14] Michal Rolínek, Paul Swoboda, Dominik Zietlow, Anselm Paulus, Vít Musil, and Georg Martius, “Deep graph matching via blackbox differentiation of combinatorial solvers,” in *ECCV*, 2020, pp. 407–424.
- [15] Qibing Ren, Qingquan Bao, Runzhong Wang, and Junchi Yan, “Appearance and structure aware robust deep visual graph matching: Attack, defense and beyond,” in *Proceedings of the IEEE/CVF Conference on Computer Vision and Pattern Recognition*, 2022, pp. 15263–15272.
- [16] Yijie Lin, Mouxing Yang, Jun Yu, Peng Hu, Changqing Zhang, and Xi Peng, “Graph matching with bi-level noisy correspondence,” *arXiv preprint arXiv:2212.04085*, 2022.
- [17] Yunsheng Shi, Zhengjie Huang, Shikun Feng, Hui Zhong, Wenjin Wang, and Yu Sun, “Masked label prediction: Unified message passing model for semi-supervised classification,” in *IJCAI*, 2021.
- [18] Thomas N Kipf and Max Welling, “Semi-supervised classification with graph convolutional networks,” *ICLR*, 2017.
- [19] Petar Veličković, Guillem Cucurull, Arantxa Casanova, Adriana Romero, Pietro Lio, and Yoshua Bengio, “Graph attention networks,” *arXiv preprint arXiv:1710.10903*, 2017.
- [20] Shaked Brody, Uri Alon, and Eran Yahav, “How attentive are graph attention networks?,” *arXiv preprint arXiv:2105.14491*, 2021.
- [21] R. Sinkhorn and A. Rangarajan, “A relationship between arbitrary positive matrices and doubly stochastic matrices,” *Ann. Math. Statistics*, 1964.
- [22] Karen Simonyan and Andrew Zisserman, “Very deep convolutional networks for large-scale image recognition,” in *ICLR*, 2014.
- [23] Kaiming He, Xiangyu Zhang, Shaoqing Ren, and Jian Sun, “Deep residual learning for image recognition,” in *CVPR*, 2016, pp. 770–778.
- [24] Kun Yuan, Shaopeng Guo, Ziwei Liu, Aojun Zhou, Fengwei Yu, and Wei Wu, “Incorporating convolution designs into visual transformers,” in *ICCV*, 2021, pp. 579–588.
- [25] Alaaeldin Ali, Hugo Touvron, Mathilde Caron, Piotr Bojanowski, Matthijs Douze, Armand Joulin, Ivan Laptev, Natalia Neverova, Gabriel Synnaeve, Jakob Verbeek, et al., “Xcit: Cross-covariance image transformers,” *NeurIPS*, 2021.